IAA-AAS-DyCoSS1 -11-03

STATION KEEPING OF A SOLAR SAIL AROUND A HALO ORBIT

Ariadna Farrés* **and Àngel Jorba†**

Solar sails are a concept of spacecraft propulsion that takes advantage of solar radiation pressure to propel a spacecraft. Although the thrust provided by a solar sail is small it is constant and unlimited. This offers the chance to deal with novel mission concept. In this work we want to discuss the controllability of a spacecraft around a Halo orbit by means of a solar sail. We will describe the natural dynamics for a solar sail around a Halo orbit. By natural dynamics we mean the behaviour of the trajectory of a solar sail when no control on the sail orientation is applied. We will then discuss how a sequence of changes on the sail orientation will affects the sail's trajectory, and we will use this information to derive efficient station keeping strategies. Finally we will check the robustness of these strategies including different sources of errors in our simulations.

INTRODUCTION

Halo orbits are placed on a privileged location, that has already been considered for several mission applications. For instance, the SOHO telescope has been orbiting around a Halo orbit near the Sun - Earth L_1 since 1995, making observation of the Sun's activity. Or Genesis, a sample return probe which collected samples of the solar wind, orbited around a Halo orbit about L_1 for several months. Recently, the James Web telescope plans to orbit a Halo orbit around L_2 to make precise observations of the deep space.

When we add the solar radiation pressure due to a solar sail, these orbits come closer to the Sun and with an appropriate sail orientation they can be tilted above and below the ecliptic plane.[1,2] Unfortunately all these orbits are highly unstable and a station keeping strategy is required to remain close to them. In this paper we want to discuss the controllability of these orbits and how to derive efficient station keeping strategies for solar sails.

To model the dynamics of a solar sail we use the Restricted Three Body Problem (RTBP) taking Earth and Sun as primaries and adding the solar radiation pressure. The force due to the sail is parameterised by its orientation, defined by two angles (α, δ), and its efficiency, given by the sail lightness number β.[3]

We will use the same ideas presented in[4,5] for the station keeping around equilibrium points to deal with the station keeping of a solar sail around a Halo orbit. We first need to understand the behaviour of the phase space around a nominal orbit and how changes on the sail orientation affect the sail's trajectory.

*Dr., Institut de Mécanique Céleste et de Calcul des Éphémérides, Observatire de Paris, 77 Avenue Denfert-Rochereau 75014 Paris, France.

†Prof., Departament de Matemàtica Aplicada i Anàlisis, Universitat de Barcelona, Gran Via de les Corts Catalanes 585, 08007 Barcelona, Spain.

We will see that the linear dynamics around a Halo orbit is a cross product between a saddle, a centre and the direction of the family of periodic orbits. If a solar sail is close to a Halo orbit (H_0) for a given fixed sail orientation $\alpha = \alpha_0$, $\delta = \delta_0$, its trajectory will escape along the unstable manifold (W_0^u) and rotate along the centre direction. When we change the sail orientation, $\alpha = \alpha_1$, $\delta = \delta_1$ the position of the Halo orbit (H_1) is shifted, as well as the stable and unstable manifolds. Now the trajectory will escape along the new unstable manifold (W_1^u).

In order to maintain the solar sail trajectory close to the nominal Halo orbit we need that the new unstable manifold (W_1^u) takes the trajectory close to the stable manifold of H_0 (W_0^s). If we can find a suitable sail orientation α_1, δ_1, then when we get close to W_0^s , we can restore the sail orientation to α_0, δ_0. The main idea is to repeat this process, finding a sequence of changes for the sail orientation that maintain the solar sail's trajectory close to a nominal Halo orbit. Nevertheless, one must not forget the contributions of these changes to the centre projections. We recall that in one of these directions we have a rotating motion around the periodic orbit. A sequence of changes on the sail orientation are a sequence of rotations around different periodic orbits on the centre projection and this can result of an unbounded growth.

We will use the first order variational equation of the flow with respect to the two angles defining the sail orientation to understand and quantify the effects of small changes on the sail orientation on the sail's trajectory. We will use this information to find appropriate changes for the sail orientation so that the trajectory of the solar sail comes close to the nominal Halo orbit, maintaining both the saddle and the centre projection bounded.

Finally we will test the robustness of these strategies around different Halo orbits. We will include different sources of error during the simulations, such as errors on the position and velocity determination and errors on the sail orientation.

EQUATIONS OF MOTION

To describe the dynamics of a solar sail in the Earth - Sun system we consider the Restricted Three Body Problem (RTBP) adding the Solar Radiation Pressure (SRP) due to the solar sail (RTBPS). We assume that the Earth and Sun are point masses moving around their common centre of mass in a circular way, and that the solar sail is a massless particle that is affected by the gravitational attraction of both bodies and the SRP. We normalise the units of mass, distance and time, so that the total mass of the system is 1, the Earth - Sun distance is 1 and the period of its orbit is 2π. We use a rotating reference system with the origin at the centre of mass of the Earth - Sun system and such that the Earth and Sun are fixed on the x-axis, the z is perpendicular to the ecliptic plane and y defines an orthogonal positive oriented reference system (see Figure 1).

The acceleration given by the solar sail depends on its orientation and its efficiency. In this paper we consider the simplest model for a solar sail: we assume it to be flat and perfectly reflecting, so the force due to the solar radiation pressure is in the normal direction to the surface of the sail,[3]

$$\vec{F}_{sail} = \beta \frac{1-\mu}{r_{PS}^3} \langle \vec{r}_s, \vec{n} \rangle^2 \vec{n}, \tag{1}$$

where β is the sail lightness number and accounts for the sail efficiency, $\vec{r}_s$ is the Sun - line direction and $\vec{n}$ is the normal direction to the surface of the sail (we note that both vectors, $\vec{n}$ and $\vec{r}_s$ have been normalised).

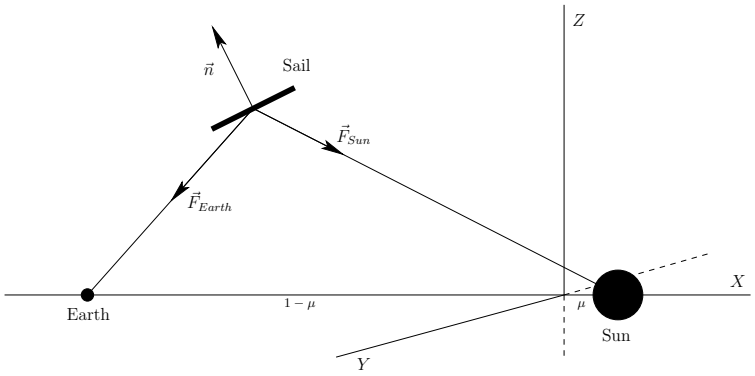

Figure 1. Schematic representation of the position of the two primaries and the solar sail in the rotating reference system.

For a more realistic model one should account for the absorption of the photons by the surface of the sail. In this case an extra component in the transverse direction of the sail must be added,[6] slightly changing the efficiency of the sail and the direction of the acceleration vector.

Within our assumptions, the equations of motion in the rotating reference system are:

$$\begin{aligned}
\ddot{X} = &\ 2\dot{Y} + X - \frac{(1-\mu)}{r_{PS}^3}(X-\mu) - \frac{\mu}{r_{PE}^3}(X-\mu+1) + \beta\frac{(1-\mu)}{r_{PS}^3}\langle\vec{r}_s,\vec{n}\rangle^2 N_X, \\
\ddot{Y} = &\ -2\dot{X} + Y - \left(\frac{(1-\mu)}{r_{PS}^3} + \frac{\mu}{r_{PE}^3}\right) Y + \beta\frac{(1-\mu)}{r_{PS}^3}\langle\vec{r}_s,\vec{n}\rangle^2 N_Y, \\
\ddot{Z} = &\ -\left(\frac{(1-\mu)}{r_{PS}^3} + \frac{\mu}{r_{PE}^3}\right) Z + \beta\frac{(1-\mu)}{r_{PS}^3}\langle\vec{r}_s,\vec{n}\rangle^2 N_Z,
\end{aligned} \tag{2}$$

with $r_{PS} = \sqrt{(X-\mu)^2+Y^2+Z^2}$ and $r_{PE} = \sqrt{(X-\mu+1)^2+Y^2+Z^2}$ the Sun - sail and Earth - sail distances respectively, $\vec{r}_s = (X-\mu, Y, Z)/r_{PS}$ and $\vec{n} = (N_X, N_Y, N_Z)$.

The sail orientation is parameterised by two angles, α and δ, which allow different definitions.[3,7,8] We define them as follows: α is the angle between the projection of the Sun - sail line, $\vec{r}_s$, and the normal vector to the sail, $\vec{n}$, on the ecliptic plane; δ is the angle between the projection of the Sun - sail line, $\vec{r}_s$, and the normal vector to the sail, $\vec{n}$, on the $y = 0$ plane.

Following these definitions we have that:

$$\begin{aligned}
N_X &= \cos(\phi(X,Y)+\alpha)\cos(\psi(X,Y,Z)+\delta), \\
N_Y &= \sin(\phi(X,Y)+\alpha)\cos(\psi(X,Y,Z)+\delta), \\
N_Z &= \sin(\psi(X,Y,Z)+\delta),
\end{aligned} \tag{3}$$

where $\phi(X,Y)$, $\psi(X,Y,Z)$ are the angles defining the Sun - sail direction $\vec{r}_s$ is spherical coordinates:

$$\phi(X,Y) = \arctan\left(\frac{Y}{X-\mu+1}\right), \qquad \psi(X,Y,Z) = \arctan\left(\frac{Z}{\sqrt{(X-\mu+1)^2+Y^2}}\right).$$

NATURAL DYNAMICS ON THE RTBPS

We know that when the radiation pressure is discarded, the RTBP has five equilibrium points: three of them ($L_{1,2,3}$) are on the axis joining the two primaries and their linear dynamics is centre $\times$ centre $\times$saddle; the other two ($L_{4,5}$) lie on the ecliptic plane forming an equilateral triangle with the two primaries and their linear dynamics is centre $\times$ centre $\times$ centre if μ is below the Routh critical value. We also know that around $L_{1,2,3}$ we find two families of unstable periodic orbits, the vertical and horizontal Lyapunov families, and a set of invariant tori. Moreover, for certain energy levels the well known family of Halo orbits appears.[9]

Before dealing with the station keeping of a solar sail around a Halo orbit let us briefly describe how the dynamics close to $L_{1,2,3}$ varies when we include the solar radiation pressure due to a solar sail.

Equilibrium Points

If we consider the sail to be perpendicular to the Sun - sail line ($\alpha = \delta = 0$), we have similar phase portrait as in the RTBP. Notice that we are essentially changing the attracting force form the Sun. The system is still Hamiltonian and has 5 equilibrium points, $SL_{1,\ldots,5}$, which are closer to the Sun than the classical $L_{1,\ldots,5}$. The dynamics around these displaced equilibria ($SL_{1,\ldots,5}$) is qualitatively the same as the one around their "brothers" $L_{1,\ldots,5}$.

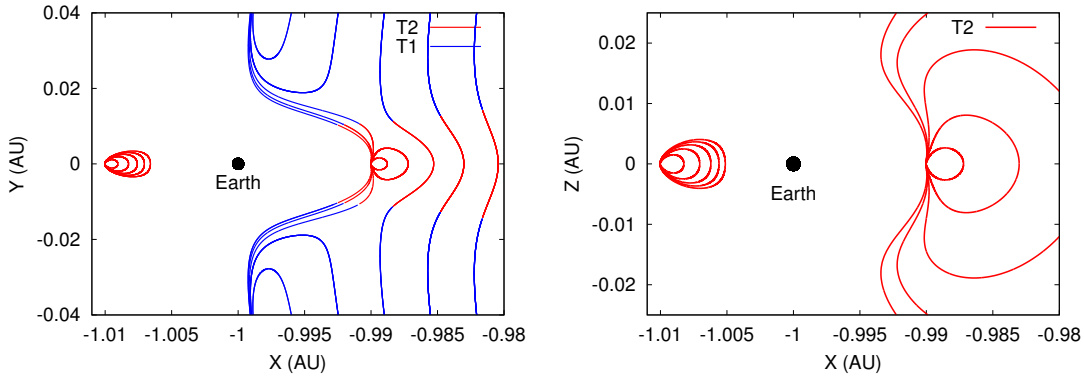

Figure 2. Position of the family of "artificial" equilibria close to L_1 and L_2 for $\beta = 0.01, 0.02, 0.03$ and 0.04. Right: Fixed points for $Z = 0$; Left: Fixed points for $Y = 0$.

When we consider a general orientation for the sail, the RTBPS is no-longer Hamiltonian. For a fixed value of the sail lightness number (β) we can displace the equilibrium point by changing the sail orientation. So, we have a 2D family of equilibrium points parameterised by the two angles that define the sail orientation.[3,10] In Figure 2 we show two slices of these families for $\beta = 0.01, 0.02, 0.03$ and 0.04.

Most of these "artificial" equilibria are linearly unstable.[10] Nevertheless, we can distinguish two kind of behaviours around these points by looking at the eigenvalues of the differential matrix of the flow at equilibria. We find two classes: $T1$ where there are 3 pair of complex eigenvalues $\gamma_{1,2,3} \pm \omega_{1,2,3}$; and $T2$ where there are 2 pair of complex eigenvalues $\gamma_{2,3} \pm \omega_{2,3}$ and a pair of real eigenvalues $\pm\lambda_1$. We note that in general $|\gamma_i|$ is small, hence we can say that the points of class $T1$ are practically stable as trajectories takes long time to escape from a close vicinity of equilibria.[5,11]

Periodic Motion

In order to find periodic and quasi-periodic motion we must restrict ourselves to the particular case of $\alpha = 0$ and $\delta \in [-\pi/2, \pi/2]$ (i.e. we only allow the sail orientation to vary vertically w.r.t. the Sun - sail line direction). In this case, the system is time-reversible by the symmetry $R : (t, X, Y, Z, \dot{X}, \dot{Y}, \dot{Z}) \to (-t, X, -Y, Z, -\dot{X}, \dot{Y}, -\dot{Z})$, which means that under certain constraints the flow will behave locally like Hamiltonian system.[12,13] This is not the case for $\alpha \neq 0$ where further studies on the non-linear dynamics around the "artificial equilibria" equilibria must be done. The reversible character of the system ensures the existence of periodic and quasi-periodic motion around the equilibrium points that lie on the $Y = 0$ plane (these are the ones in Figure 2 left). We note that the linear dynamics around all of these points is centre $\times$ centre $\times$ saddle.

Around each of these "artificial" equilibrium points we can distinguish two families of periodic orbits each one related to one of the oscillations given by the linear approximation. For δ small, one of the two complex eigendirections has a wider vertical oscillation than the other. From now on we call the *$\mathcal{P}$-Lyapunov family* to the family of periodic orbits emanating from an equilibrium point p_0 whose planar oscillation is wider that the vertical one and *$\mathcal{V}$-Lyapunov family* to the other family of periodic orbits.[14] We can compute these families of periodic orbits by means of a continuation methods.

$\mathcal{P}$-Lyapunov family of periodic orbits. The orbits in this family are all transverse to the plane $Y = 0$. We use the Poincaré section $\Gamma_1 = \{Y = 0, \dot{Y} > 0\}$ to compute these orbits as fixed points on Γ_1 and use the variable X of these points on the section as the continuation parameter. In Figure 3 we see the continuation scheme for $\delta = 0$ (left) and $\delta = 0.01$ (right). On the horizontal axis we have the continuation parameter X and on the vertical axis we have the Z component of the periodic orbit on Γ_1.

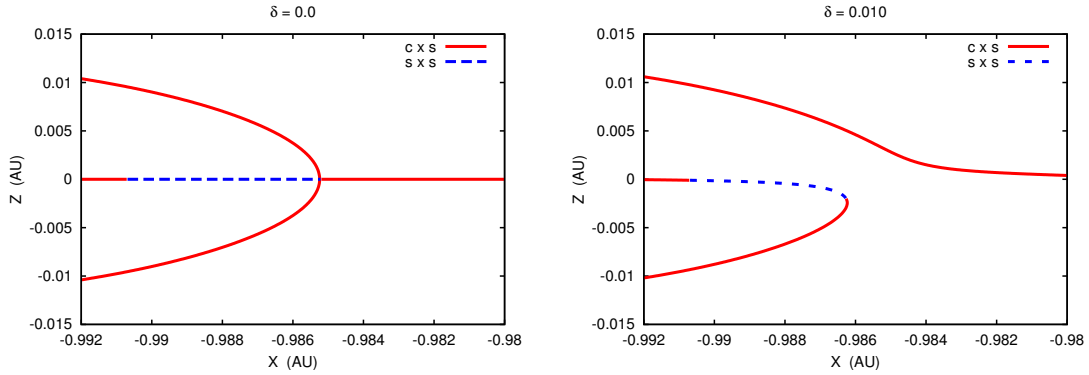

Figure 3. Bifurcations scheme for the continuation of periodic orbits w.r.t. X_0 for the Planar family of periodic orbits for $\delta = 0$ (left) and $\delta = 0.01$ (right). Where, continuous line (`c x s`): saddle $\times$ centre periodic orbits, and dashed line (`s x s`): saddle $\times$ saddle periodic orbits.

For $\delta = 0$, the family of periodic orbits emanating from p_0 are totally contained in the $Z = 0$ plane, and are centre $\times$ saddle. At a certain point, a pitchfork bifurcation takes place and two new families periodic orbits are born. These orbits are the Halo orbits for a solar sail when the sail is perpendicular to the Sun - sail line.

For $\delta \neq 0$, the family of periodic orbits emanating from p_0 are no longer contained in the $Z = 0$ plane, but for δ small they are almost planar. Now, there is no longer a pitchfork bifurcation, the

two branches have split due to a symmetry breaking on the system for $\delta \neq 0$.[15] Nevertheless, we still find families of Halo - type orbits that persist.

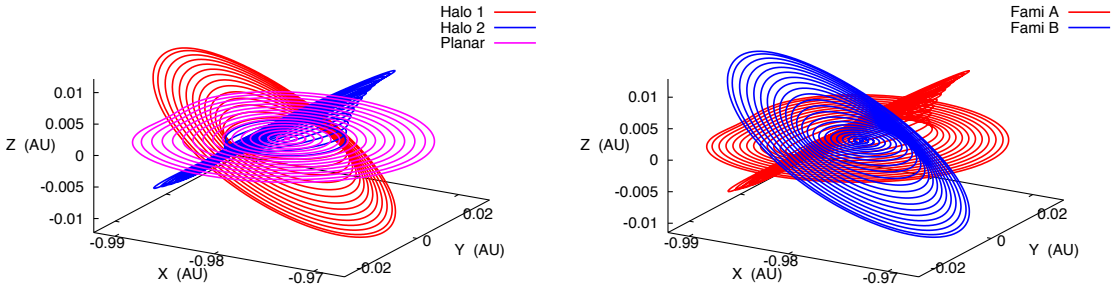

Figure 4. Projections of the $\mathcal{P}$-Lyapunov family of periodic orbits close to SL_1 for $\beta = 0.05$ and $\delta = 0$ (left), $\delta = 0.01$ (right).

In Figure 4 we show the X, Y, Z projections of these families of periodic orbits for $\delta = 0$ and $\delta = 0.01$. We can see that the qualitative behaviour of the phase space does not vary much for $\alpha = 0$ and δ small.

$\mathcal{V}$-Lyapunov family of periodic orbits. The orbits in this family cross transversely the planes $Y = 0$ and $Z = Z^*$, (Z^* is the Z component of the equilibrium point for a given sail orientation $\alpha = 0, \delta = \delta_0$). We use the Poincaré section $\Gamma_2 = \{Z = Z^*, \dot{Z} > 0\}$ to continue these families and the X component of the orbit on the section Γ_2 as the continuation parameter. We see that for a low orbits no bifurcation appears and all of these orbits are centre $\times$ saddle.

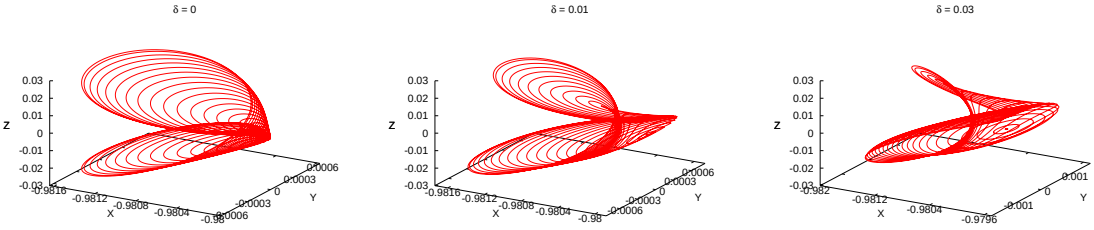

Figure 5. Projections on the X, Y, Z plane of the $\mathcal{V}$ Family of periodic orbits for $\delta = 0, \delta = 0.005, \delta = 0.01$ and $\delta = 0.03$ (SL1)

In Figure 5 we can see 3D projections of these families for equilibrium points close to SL_1 with $\delta = 0, 0.01$ and 0.03. Notice that when $\delta = 0$ these orbits have a bow-tie shape symmetric with respect to the $Z = 0$ plane. When $\delta \neq 0$ the periodic orbits on the family that are close to the equilibrium are almost circular, and as we move along the family their shape changes taking also a bow-tie shape. Although now there is no symmetry between the two loops.

HALO ORBITS FOR SOLAR SAILS

As we have mentioned in the previous section, despite the extra effect of the SRP due to the solar sail, we still find families of Halo - type orbits around $SL_{1,2,3}$ for different fixed sail orientations. The Halo orbits around SL_1 offer a unique position in the Earth-Sun system, and can be used for observing the Sun, such as SOHO. As these orbits are closer to the Sun than the classical Halo orbits

they can provide enhanced warning on the Sun's geomagnetic activity. On the other hand, the Halo orbits around SL_2 can be used for observations of the deep sky, in mission concepts like GAIA or the James Webb Space Telescope. Nevertheless, as in the RTBP all these orbits are unstable and an active control is required to remain close to them.

Before deriving a station keeping strategy for solar sails around Halo - type orbits, let us discuss the natural dynamics of the system around these orbits, and how changes on the sail orientation can affect the trajectory of the solar sail.

Linear dynamics around a Halo orbit

The study of the local behaviour around a periodic orbit is usually done throughout the first order variational equations. To fix notation, let us denote by ϕ the flow associated to the equations of motion. Then $\phi_\tau(x_0)$ the image of the point $x_0 \in \mathbb{R}^6$ at $t = 0$ at a time $t = \tau$, and $A(\tau) = D\phi_\tau(x_0)$ is the first order variational of $\phi_\tau(x_0)$ with respect to the initial condition (x_0). For $h \in \mathbb{R}^6$, we have

$$\phi_\tau(y_0 + h) = \phi_\tau(y_0) + D\phi_\tau(y_0) \cdot h + O(|h|^2).$$

Hence, $\phi_\tau(y_0) + A(\tau) \cdot h$ gives a good approximation of $\phi_\tau(y_0 + h)$ provided h small. The linear dynamics around a periodic orbit is given by the study of the eigenvalues and eigenvectors of the monodromy matrix of the orbit $A(T)$, where T is the period of the orbit.

One can check that the eigenvalues $(\lambda_{1,\dots,6})$ of the monodromy matrix, $A(T)$, of the Halo - type orbits described previously satisfy: $\lambda_1 > 1, \lambda_2 < 1$, $\lambda_3 = \bar{\lambda}_4$ are complex with modulus 1 and $\lambda_5 = \lambda_6 = 1$. These three pairs of eigenvalues and their associated eigenvectors have the following geometrical meaning:[16]

- The first pair (λ_1, λ_2), verify $\lambda_1 \cdot \lambda_2 = 1$, and are related to the hyperbolic character of the orbit. The value λ_1 is the largest in absolute value, and is related to the eigenvector $e_1(0)$, which gives the most expanding direction. After one period, a given distance to the nominal orbit in this direction is amplified in a factor of λ_1. Using $D\phi_\tau$ we can get the image of this vector under the variational flow: $e_1(\tau) = D\phi_\tau e_1(0)$. At each point of the orbit, the vector $e_1(\tau)$ together with the vector tangent to the orbit, span a plane that is tangent to the local unstable manifold (W^u_{loc}). In the same way λ_2 and its related eigenvector $e_2(0)$ are related to the stable manifold and $e_2(\tau) = D\phi_\tau e_2(0)$.

- The second pair (λ_3, λ_4) are complex conjugate eigenvalues of modulus 1. Together with the other two eigenvalues equal to 1 describe the central motion around the periodic orbit. The monodromy matrix restricted to the plane spanned by the real $(e_3(0))$ and imaginary $(e_4(0))$ parts of the eigenvectors associated to λ_3, λ_4 along the orbit is a rotation of angle $\Gamma = \arctan\left(\frac{\mathrm{Im}\,(\lambda_3)}{\mathrm{Re}\,(\lambda_3)}\right)$, the argument of λ_3.

- The third couple $(\lambda_5, \lambda_6) = (1, 1)$, is associated to the neutral directions (i.e. non-unstable modes). There is only one eigenvector of $A(T)$ with eigenvalue 1, this vector is the tangent vector to the orbit and we call it $e_5(0)$. The other eigenvalue is associated to variations of the period or any other variable which parameterised the family of periodic orbits. The related eigenvector is chosen orthogonal to $e_5(0)$ in the 2D space associated to the eigenvalue 1, and gives the tangent direction to the family of Halo orbits. The monodromy matrix restricted to

this plane has the form

$$\begin{pmatrix} 1 & \varepsilon \\ 0 & 1 \end{pmatrix}.$$

The fact that ε is not zero is due to the variation of the period along the family of Halo orbits.

To sum up, we can state that, in the basis given by $(e_1(0), \ldots, e_6(0))$, the monodromy matrix associated to a Halo - type orbit is written in the form,

$$J = \begin{pmatrix} \lambda_1 & & & & & \\ & \lambda_2 & & & & 0 \\ & & \cos\Gamma & -\sin\Gamma & & \\ & & \sin\Gamma & \cos\Gamma & & \\ & 0 & & & 1 & \varepsilon \\ & & & & 0 & 1 \end{pmatrix}.$$

and the functions $e_i(\tau) = D\phi_\tau \cdot e_i(0)$, $i = 1, \ldots, 6$, gives an idea of the variation of the phase space properties in a small neighbourhood of the periodic orbit.

We can define $e_i(\tau) = D\phi_\tau e_i(0)$ as a reference system centred around the periodic orbit, $\phi_\tau(x_0)$, where the dynamics around a Halo orbit is simple: along the planes generated by $e_1(\tau), e_2(\tau)$ the trajectory will escape with an exponential rate along the unstable direction $(e_1(\tau))$; on the planes generated by $e_3(\tau), e_4(\tau)$ the dynamics is a rotation around the periodic orbit; and on the planes generated by $e_5(\tau), e_6(\tau)$ the dynamics is neutral.

Effects of small changes in the sail orientation

We recall that for $\alpha = 0, \delta \neq 0$ but small we find families of Halo - type orbits that are slightly displaced one from the other for different values of δ. Moreover, the linear dynamics around these orbits is qualitatively the same.

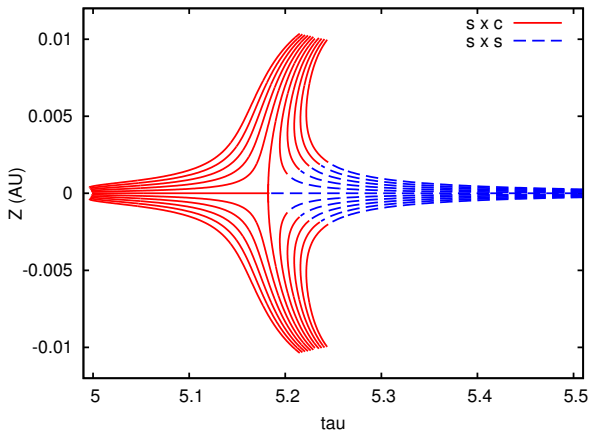

Figure 6. Bifurcations scheme for the continuation of periodic orbits w.r.t. τ for the Planar family of periodic orbits for $\delta = 0, \pm 0.002, \pm 0.004, \pm 0.006, \pm 0.008, \pm 0.01$. The continuous line (`c x s`): saddle $\times$ centre periodic orbits, and dashed line (`s x s`): saddle $\times$ saddle periodic orbits.

In Figure 6 we show the continuation scheme of these families of orbits. Each point corresponds to the point of the periodic orbit on the Poincaré section $\Gamma = \{Y = 0, \dot{Y} > 0\}$. On the horizontal line we plot the continuation parameter, the period of the orbit τ, and on the vertical axis the Z amplitude of these orbits on the Poincaré section. We show the continuation curves for $\beta = 0.05$ and $\delta = 0, \pm 0.002, \pm 0.004, \pm 0.006, \pm 0.008, \pm 0.01$.

As we can see the position of low amplitude Halo orbits varies more with respect to variations on δ than for large amplitude Halo orbits. Also, low amplitude Halo orbits are close to bifurcations, where orbits change from centre $\times$ saddle to saddle $\times$ saddle. This will complicate the station keeping around them.

Now, let us suppose that the solar sail is close to a nominal Halo orbit with a fixed sail orientation $\alpha = 0, \delta = \delta_0$. We know that the trajectory will escape along the unstable direction and rotate around the nominal orbit on the centre projection. If we change the sail orientation $\alpha = 0, \delta = \delta_1$, the phase space portrait is shifted: the family of Halo - type orbits has been displaced and their eigenvalues and eigendirections are slightly different. Now the solar sail will escape along the unstable direction of the new Halo orbit. With an appropriate choice of δ the trajectory can come close to the nominal Halo orbit.

For the moment we have just discussed what happens if we consider changes on the sail orientation keeping $\alpha = 0$, but what happens if we take $\alpha \neq 0$? We have already mentioned that the system is no-longer time reversible and that we cannot ensure the existence of periodic and quasi-periodic motions. We know that the spectra of the equilibria for α small is $\{\lambda_1, \lambda_2, \gamma_1 \pm \omega_1, \gamma_2 \pm \omega_2\}$, with $\lambda_1 > 0, \lambda_2 < 0$, $\gamma_1 \cdot \gamma_2 < 0$ and $|\gamma_i| \ll \lambda_1$. Hence, the linear dynamics around these equilibrium points is a cross product of a saddle, a source and a sink. The source and sink ensures us that there are no families of periodic orbits emanating from the equilibrium point. But if $|\gamma_i|$ is very small we can find trajectories that almost close after one revolution. Nevertheless, the hyperbolic character of the region for $\alpha \neq 0$ is preserved when we consider the non-linear dynamics. So by varying α we can still have stable and unstable directions that drive the trajectories back to the nominal periodic orbit.

A comment on the station keeping strategy

As we have already mentioned, our final goal is to derive station keeping strategies for a solar sail around Halo orbits. The key point of these strategies is to understand the geometry of the phase space close to a Halo orbit and how it is affected for small variations on the sail orientation. With this knowledge we can try to find appropriate changes on the sail orientation such that the phase space acts in our favour, keeping the trajectory close to the desired Halo orbit.

We recall that if the solar sail is close to a nominal Halo orbit (H_0) with a fixed sail orientation $\alpha = 0, \delta = \delta_0$, the trajectory will escape along the unstable direction. To control the instability given by the saddle, we want to find a new sail orientation, such that the new unstable manifold brings the trajectory close to the stable manifold of the nominal Halo orbit. Then we can restore the initial sail orientation ($\alpha = 0, \delta = \delta_0$) and let the dynamics act. We can repeat this process over and over to keep the hyperbolic projection bounded. Nevertheless, we must not forget the projection of the trajectory in two the centre directions. Let us now discuss how a sequence of changes on the sail orientation affects the projection of the trajectory on the two centre directions.

We recall that the motion in the directions $e_3(\tau), e_4(\tau)$ is a rotation around the periodic orbit. A sequence of changes on the sail orientation would derive on a sequence of rotations around different

periodic orbits, which if we do not control, can result in an unbounded growth.[4]

The motion in the directions $e_5(\tau), e_6(\tau)$ is neutral and gives us an idea of the position of the trajectory with respect to the orbits in the family. Here sequences of changes on the sail orientation could derive in a drift along the orbits in the family.

To this point, it is not obvious that we will always be able to find appropriate changes on the sail orientation to remain close to the nominal Halo orbit. First we need to quantify the effect that small changes on the sail orientation have on the sail trajectory. Then we use this information to find the appropriate changes on the sail orientation to derive efficient station keeping strategies.

First order variational flow

The first order variational flow gives us information on how small variations in the initial conditions affect the trajectory. In the same way the first order variational w.r.t. the two angles defining the sail orientation gives us the information on how small variations on the sail orientation affect the trajectory.

We call $\phi_{\Delta t}(t_0, x_0, \alpha_0, \delta_0)$ to the flow at time $t_1 = t_0 + \Delta t$ of the vector field starting at $t = t_0$ with $(x = x_0, \alpha = \alpha_0, \delta = \delta_0)$, and $\mathcal{F}(\Delta t, \Delta\alpha, \Delta\delta)$ to the first order approximation of $\phi_h(t_0, x_0, \alpha_0 + \Delta\alpha, \delta_0 + \Delta\delta)$,

$$\mathcal{F}(\Delta t, \Delta\alpha, \Delta\delta) = \phi_{\Delta t}(t_0, x_0, \alpha_0, \delta_0) + \frac{\partial \phi_{\Delta t}}{\partial \alpha}(t_0, x_0, \alpha_0, \delta_0)\cdot\Delta\alpha + \frac{\partial \phi_{\Delta t}}{\partial \delta}(t_0, x_0, \alpha_0, \delta_0)\cdot\Delta\delta. \quad (4)$$

Notice that $\mathcal{F}(\Delta t, \Delta\alpha, \Delta\delta)$ is a linear application that for a given $(t_0, x_0, \alpha_0, \delta_0)$ gives us a first order approximation of the position of the trajectory at time $t = t_0 + \Delta t$ if we apply a change $(\Delta\alpha, \Delta\delta)$ on the sail orientation at time $t = t_0$. We can use this application to find the appropriate change $(\Delta\alpha, \Delta\delta)$ that after a given time Δt will bring the trajectory close to the nominal orbit.

STATION KEEPING STRATEGY

Let us now give the details on the station keeping strategies for a solar sail around Halo orbits. We use ideas based on the previous works by Gómez et al.[16,17] on the station keeping around a Halo orbits with a "traditional" thrust and by Farrés et al.[4,5] on the station keeping of a solar sail around an equilibrium point.

During the station keeping strategy it is important to track the position of the trajectory with respect to the stable and unstable manifolds to know when and how we are escaping and also where we want the new sail orientation to lead the trajectory of the solar sail. We will use the *Floquet modes* to have a good reference system along the Halo orbit.

The main idea behind this strategy is to let the natural dynamics of the system act, so the trajectory escapes along the unstable manifold. When the trajectory of the solar sail is too far from the orbit, we choose an appropriate new sail orientation so that the trajectory will come close to the stable manifold of the nominal Halo orbit keeping the centre projections small. We use the linear map $\mathcal{F}(\Delta t, \Delta\alpha, \Delta\delta)$ to find this appropriate new sail orientation.

We must mention that the strategy that we describe here uses information from the linear dynamics of the system to make decisions on the changes of the sail orientation. Nevertheless, the complete set of equations are taken into account during the simulations.

The reference system

We recall that the functions $e_i(\tau) = D\phi_\tau \cdot e_i(0)$, $i = 1, \ldots, 6$, give us an idea of the behaviour of the trajectory of a solar sail in three reference planes that vary along the periodic orbit. Instead of them it is more convenient to use the *Floquet modes* $\bar{e}_i(\tau)$, $i = 1, \ldots, 6$. Six T-periodic functions that can easily be recovered from $e_i(\tau)$.[16]

The advantage of the Floquet modes is that they can be spanned as a Fourier series and easily stored by their Fourier coefficients. Moreover, we can consider the T-periodic matrix $P(t)$, that has the Floquet modes $\bar{e}_i(\tau)$ as columns. Then, the change of variables $y = P(t)z$, takes the linearization of equations of motion around a T-periodic orbit, $\dot{y} = A(\tau)y$, to an equation with constant coefficients $\dot{z} = Jz$.

Moreover, the Floquet modes give us a reference system that is very useful to track, at all time, the relative position between the spacecraft trajectory and the local unstable and stable invariant manifolds of the nominal orbit.

Following Gomez et al.,[16] we define the first and second Floquet mode taking into account that the rate of escape and approach, to the Halo orbit, along the unstable and stable manifolds is exponential:

$$\begin{aligned} \bar{e}_1(\tau) &= e_1(\tau) \exp\left(-\tfrac{\tau}{T} \ln \lambda_1\right), \\ \bar{e}_2(\tau) &= e_2(\tau) \exp\left(-\tfrac{\tau}{T} \ln \lambda_2\right). \end{aligned}$$

The third and fourth modes are computed considering that the monodromy matrix restricted to the plane generated by the real and imaginary parts of the eigenvectors associated to λ_3 and λ_4 is a rotation of angle Γ:

$$\begin{aligned} \bar{e}_3(\tau) &= \cos\left(-\tfrac{\Gamma\tau}{T}\right) e_3(\tau) - \sin\left(-\tfrac{\Gamma\tau}{T}\right) e_4(\tau), \\ \bar{e}_4(\tau) &= \sin\left(-\tfrac{\Gamma\tau}{T}\right) e_3(\tau) + \cos\left(-\tfrac{\Gamma\tau}{T}\right) e_4(\tau). \end{aligned}$$

Finally, the fifth mode is the vector tangent to the Halo orbit, and the sixth mode is chosen orthogonal to $\bar{e}_5(\tau)$ in the plane spanned by $e_5(\tau)$ and $e_6(\tau)$:

$$\begin{aligned} \bar{e}_5(\tau) &= e_5(\tau), \\ \bar{e}_6(\tau) &= e_6(\tau) - \epsilon(\tau)\bar{e}_5(\tau). \end{aligned}$$

In this new set of coordinates, the dynamics around a Halo orbit is the same as if we consider the functions $e_i(\tau)$ as a reference system. We recall that along the planes generated by $\bar{e}_1(\tau), \bar{e}_2(\tau)$ the trajectory escapes along the unstable direction $\bar{e}_1(\tau)$. On the planes generated by $\bar{e}_3(\tau), \bar{e}_4(\tau)$ the trajectory rotates around the periodic orbit, and, on the planes generated by $\bar{e}_5(\tau), \bar{e}_6(\tau)$ the dynamics is neutral.

The control algorithm

We always start with the solar sail close to the nominal orbit $N_0(t)$ for a fixed sail orientation $\alpha = 0, \delta = \delta_0$, and we take the reference system $\{N_0(t); \bar{e}_i(t)\}_{i=1,\ldots,6}$, where $\bar{e}_i(t)$ are the Floquet modes described above. We use this reference system to track the trajectory and take decisions on when and how to change the sail orientation.

To fix notation, if $\varphi(t_0)$ is the position and velocity of the solar sail at time t_0, then in this reference system,

$$\varphi(t_0) = N_0(t_0) + \sum_{i=1}^{6} s_i(t_0)\bar{e}_i(t_0).$$

For each mission we must define 3 parameters (ε_{max}, dt_{min} and dt_{max}) which will depend on the mission requirements and the dynamics of the system around the nominal orbit ($N_0(t)$). We define these parameters as: ε_{max} is the maximum distance to the stable direction allowed, used to decide when we change the sail orientation; dt_{min} and dt_{max} are the minimum and maximum times allowed between manoeuvres.

During the station keeping we proceed as follows. When we are close to $N_0(t_0)$ we set the sail orientation $\alpha = 0, \delta = \delta_0$. Due to the saddle, the trajectory escapes along the unstable direction. When $|s_1(t_1)| > \varepsilon_{max}$, we say that the sail is about to escape so we need to change the sail orientation. We use the first order variational flow application $\mathcal{F}(\Delta t, \Delta\alpha, \Delta\delta)$ (see Eq. (4)) to find the new sail orientation α_1, δ_1 and time $dt_1 \in [dt_{min}, dt_{max}]$ so that by changing the sail orientation now, $t = t_1$, then at a certain time $t = t_1 + dt_1$ the sail trajectory will be close to the nominal orbit, $N_0(t_1 + dt_1)$. Finally, at $t_1 + dt_1$ we will restore the sail orientation to $\alpha = 0, \delta = \delta_0$ and repeat this process during the mission lifetime.

Finding α_1, δ_1 and dt_1

Let us assume that we have $|s_1(t_1)| > \varepsilon_{max}$ at time $t = t_1$ and we need to chose a new sail orientation. We recall that $\mathcal{F}(\Delta t, \Delta\alpha, \Delta\delta)$ is a linear map that shows us how a small change in the sail orientation $(\Delta\alpha, \Delta\delta)$ at $t = t_1$ affects the sail trajectory at time $t = t_1 + \Delta t$.

We want to find $\Delta\alpha_1, \Delta\delta_1$ and dt_1 so that the flow at time $t = t_1 + dt_1$ is close to the stable manifold, i.e. $|s_1(t_1 + dt_1)|$ small, and the centre projections, $(s_3(t_1 + dt_1), s_4(t_1 + dt_1))$ and $(s_5(t_1 + dt_1), s_6(t_1 + dt_1))$, do not grow.

We will proceed as follows:

1. Let us take $\tilde{t_i}$ for $i = 0, \ldots, n$ in the time interval $[t_1 + dt_{min}, t_1 + dt_{max}]$ where $\tilde{t_i} = t_1 + dt_{min} + i \cdot dt$ and $dt = (dt_{max} - dt_{min})/n$. For each $\tilde{t_i}$ we compute the variational map given by Eq. (4).

2. For each $\tilde{t_i}$ we try to find $\Delta\alpha_i, \Delta\delta_i$ such that, $s_1(\tilde{t_i}) = s_5(\tilde{t_i}) = s_6(\tilde{t_i}) = 0$. Notice that this reduces to solving a linear system with 2 unknowns and 3 equations, which we solve using the least square method.

   At the end we have a set of $\{\tilde{t_i}, \Delta\alpha_i, \Delta\delta_i\}_{i=1,\ldots,n}$ such that, $||(s_1(\tilde{t_i}), s_5(\tilde{t_i}), s_6(\tilde{t_i}))||$ is small.

3. From the set of $\{\tilde{t_i}, \Delta\alpha_i, \Delta\delta_i\}_{i=1,\ldots,n}$ found in step 2 we choose $\tilde{t_j}, \Delta\alpha_j, \Delta\delta_j$ such that $||(s_3(\tilde{t_j}), s_4(\tilde{t_j}))||$ is as small as possible.

Hence, the parameters that brings the sail back to the nominal orbit are:

$$\alpha_1 = \Delta\alpha_j, \quad \delta_1 = \delta_0 + \Delta\delta_j, \quad dt_1 = \tilde{t_j} - t_1. \tag{5}$$

MISSION APPLICATION

As an example to test we have considered a solar sail with a lightness number $\beta = 0.05$, which is considered to be reasonable for a short term mission application.[3] We have applied this station keeping strategy to two different Halo orbits around SL_1, both for a sail oriented perpendicular to the Sun line ($\alpha = \delta = 0$). One with a vertical displacement of 200.000km and the other of 800.000km. We want to compare the performance of our strategies between low and large amplitude orbits. We expect the strategy to be more robust for large amplitude orbits.

For each Halo orbit we will perform a Monte Carlo simulation, taking 1000 initial conditions chosen in a random way. For each initial condition the control strategy has been applied during 20 orbit revolutions. We have also measured the minimum time between manoeuvres and the maximum and minimum variations of the sail orientation ($\Delta\alpha, \Delta\delta$).

We also have tested the robustness of this strategy against different sources of errors. We have included errors in the position and velocity determination of the solar sail, as well as errors on the sail orientation each time a manoeuvre is required.

We have assumed that all the errors follow a normal distribution with zero mean. We have considered a precision on the position of the probe of $\approx$ 1m in the space slant and $\approx 2-3$milli-arc-seconds in the angle determination of the probe. The precision in speed is $\approx 20-30$microns/seconds. These errors are introduced every time the control algorithm asks the position and velocity of the solar sail to decide if a manoeuvre should or not be done. As we will see the effects of these errors turn out to be almost negligible to the controllability of the probe.

The errors on the sail orientation have an important effect on the sail trajectory and its controllability. We have included errors on the sail orientation each time the sail orientation is changed ($\alpha = \alpha_1 + \epsilon_\alpha$, $\delta = \delta_1 + \epsilon_\delta$). We have also assumed that these errors follow a normal distribution with zero mean, and we have tested the strategies for different precision of 0.001° and 0.01°.

Halo Orbit ($\Delta Z = 200.000$**km)**

Here we present the results for a Halo orbit with a vertical displacement of $\approx$ 200.000km. In dimensionless coordinates the point of the periodic orbit in the Poincaré section Γ_1 satisfies: $X_0 = -0.9856341433412470$, $Z_0 = 0.0012742447292122$, $Y_0' = 0.0139154953642598$. This orbit has a period of ≈ 301.27 days.

We recall that to apply the station keeping strategy we need to define 3 mission parameters that are used each time we need to find a new sail orientation: $\varepsilon_{max}, dt_{min}, dt_{max}$. Here we present the results considering an escape distance: $\varepsilon_{max} = 5 \cdot 10^{-5}$AU $\approx$ 7479.9km and $\varepsilon_{max} = 10^{-5}$AU $\approx$ 1495.98km; a minimum and maximum time between manoeuvres: $dt_{min} = 30$ days and $dt_{max} = 115$ days.

In Table 1 we summarise the results for the different Monte Carlo simulations. For each simulations we show the $\%$ of trajectories that remain close to the nominal Halo orbit after 20 orbital revolutions and the maximum and minimum variations on the two angles defining the sail orientation. The first two lines show the results when we do not consider errors during the simulations. The other four lines are for simulations considering errors in the position and velocity determination as well as errors on the sail orientation. `Err 1` shows the results for $\epsilon_\alpha = \epsilon_\delta = 0.001^\circ$ and `Err 2` the results for $\epsilon_\alpha = \epsilon_\delta = 0.01^\circ$.

As we can see, the maximum variation of the sail orientation is related to ε_{max}. We use larger

Table 1. Statistics for the simulations of the station keeping around a Halo orbit with $\Delta Z = 200.000$km. Different magnitudes on the error for the sail orientation are considered: `Err 1` $\rightarrow \epsilon_{\alpha,\delta} = 0.001°$, `Err 2` $\rightarrow \epsilon_{\alpha,\delta} = 0.01°$.

Sim. type	% Succ.	ε_{max} (AU)	$\Delta\alpha$ (deg)	$\Delta\delta$ (deg)
`No Err`	100 %	10^{-5}	`0.045 - 0.001`	`0.047 - 0.001`
`No Err`	85.4 %	$5 \cdot 10^{-5}$	`0.216 - 0.001`	`0.239 - 0.001`
`Err 1`	100 %	10^{-5}	`0.049 - 0.001`	`0.051 - 0.001`
`Err 1`	83.6 %	$5 \cdot 10^{-5}$	`0.219 - 0.001`	`0.244 - 0.001`
`Err 2`	18.7 %	10^{-5}	`0.125 - 0.001`	`0.115 - 0.001`
`Err 2`†	70.8 %	$5 \cdot 10^{-5}$	`0.272 - 0.001`	`0.262 - 0.001`

changes on the sail orientation for larger values of ε_{max}, which will imply more robustness of the strategies towards errors on the sail orientation. Nevertheless, as we have discussed in previous sections, dynamics close to low Halo orbits is sensitive to small variations of δ. This is why when no errors are taken into account we manage to control all the trajectories for $\varepsilon_{max} = 10^{-5}$ and not for $\varepsilon_{max} = 5 \cdot 10^{-5}$.

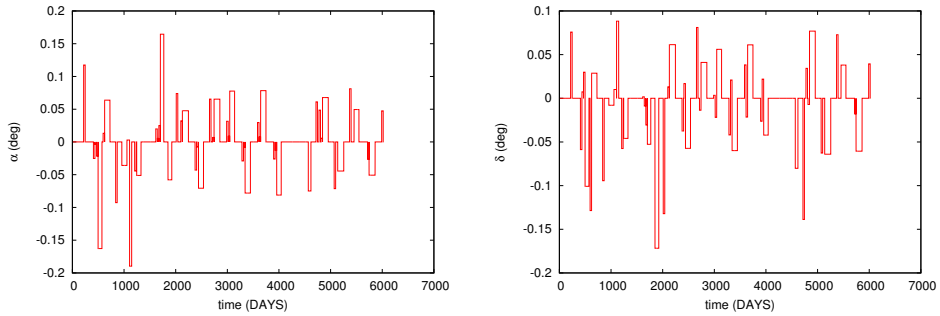

Figure 7. Simulation with no errors for a Halo orbit with $\Delta Z = 200.000$km. Variation of the sail orientation withe respect to time.

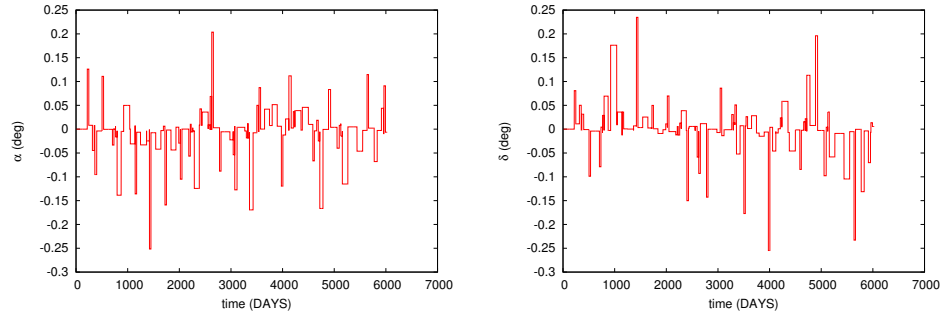

Figure 8. Simulation with errors for a Halo orbit with $\Delta Z = 200.000$km. Variation of the sail orientation withe respect to time.

We include some figures to show the control on the sail orientation and the trajectory that the solar sail follows during one simulation. We include a simulation when no errors are considered and another one when both sources of errors are taken into account with $\epsilon_{\alpha,\delta} = 0.01°$. Figures 7 and 9 show results for a simulation where no errors are considered and Figures 8 and 10 show the results for a simulation with errors.

Figures 7 and 8 show the variation of the sail orientation along time with and without errors.

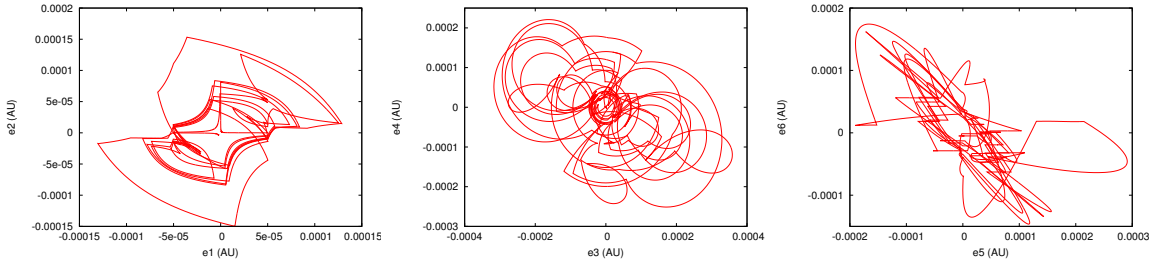

Figure 9. Simulation with no errors for a Halo orbit with $\Delta Z = 200.000$km. Trajectory in the Floquet reference system: Saddle projection $\{\bar{e}_1(\tau), \bar{e}_2(\tau)\}$ (left); Centre projection $\{\bar{e}_3(\tau), \bar{e}_4(\tau)\}$ (middle); Neutral projection $\{\bar{e}_5(\tau), \bar{e}_6(\tau)\}$ (right).

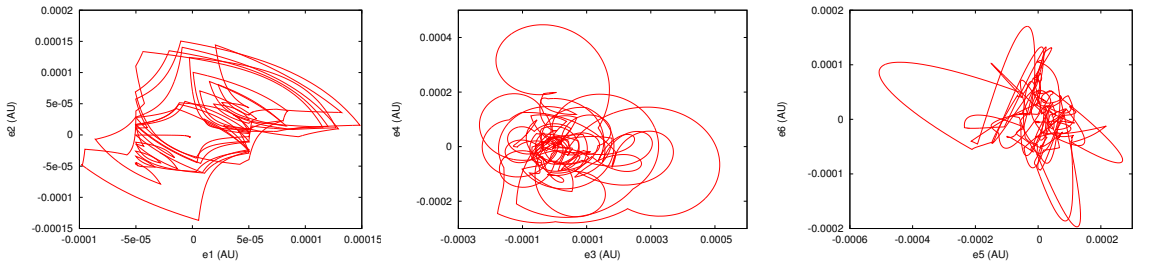

Figure 10. Simulation with errors† for a Halo orbit with $\Delta Z = 200.000$km. Trajectory in the Floquet reference system: Saddle projection $\{\bar{e}_1(\tau), \bar{e}_2(\tau)\}$ (left); Centre projection $\{\bar{e}_3(\tau), \bar{e}_4(\tau)\}$ (middle); Neutral projection $\{\bar{e}_5(\tau), \bar{e}_6(\tau)\}$ (right).

Notice that the average variation of the sail orientation in both simulations is $\Delta\alpha \approx 0.1^\circ$ and $\Delta\delta \approx 0.05^\circ$. The main difference between both simulations is that when errors are considered, we find more abrupt changes from time to time to correct the escape trajectory induced by the errors on the sail orientation.

Figures 9 and 10 show the projection of the trajectory in the Floquet reference system. Notice that the trajectory in the saddle projection $\{\bar{e}_1(\tau), \bar{e}_2(\tau)\}$ is a sequence of saddle connections; the centre projection $\{\bar{e}_3(\tau), \bar{e}_4(\tau)\}$ is a sequence of rotations around different points; and the neutral projection $\{\bar{e}_5(\tau), \bar{e}_6(\tau)\}$ illustrates the drift of the trajectory along the family.

When no errors are taken into account the projection on the saddle direction remains almost always bounded between $[-\varepsilon_{max}, \varepsilon_{max}]$. Due to the sensitivity of the orbits to small variations on the sail orientation, in some cases the trajectory does not come back close enough to the stable manifold, requiring extra control stages. This can derive in orbits that escape when errors on the sail orientation are taken into account. Taking ε_{max} smaller would improve the results, but then smaller changes in the sail orientation must be considered.

Finally, Figure 11 shows the trajectory that the sail follows in the position space when we consider both sources of errors in the simulations. Here we can see clearly how the trajectory remains close to the Halo orbit for the 20 orbit revolutions that we have simulated.

Halo Orbit ($\Delta Z = 800.000$km)

Here we present the results for a Halo orbit with a vertical displacement of ≈ 800.000km. In dimensionless coordinate the point of the periodic orbit in the Poincaré section Γ_1 satisfies: $X_0 = -0.9871209122349056, Z_0 = 0.0053058721104492, Y_0' = 0.0170744442223721$. This orbit has a

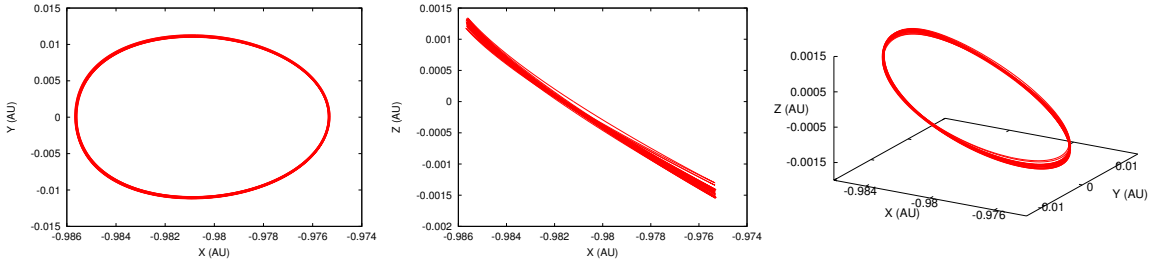

Figure 11. Simulation with errors for a Halo orbit with $\Delta Z = 200.000$km. Trajectory in the rotation reference system, XY projection (left), XZ projection (middle) and XYZ projection (right).

period of ≈ 301.83 days.

We recall that to apply the station keeping strategy we need to define 3 mission parameters that are used each time we need to find a new sail orientation: ε_{max}, dt_{min}, dt_{max}. Here we present the results considering an escape distance: $\varepsilon_{max} = 5 \cdot 10^{-5}$AU ≈ 7479.9km and $\varepsilon_{max} = 10^{-5}$AU ≈ 1495.98km; a minimum and maximum time between manoeuvres: $dt_{min} = 30$ days and $dt_{max} = 115$ days.

Table 2. Statistics for the simulations of the station keeping around a Halo orbit with $\Delta Z = 800.000$km. Different magnitudes on the error for the sail orientation are considered: `Err 1` $\rightarrow \epsilon_{\alpha,\delta} = 0.001°$, `Err 2` $\rightarrow \epsilon_{\alpha,\delta} = 0.01°$.

Sim. type	% Succ.	ε_{max} (AU)	$\Delta\alpha$ (deg)	$\Delta\delta$ (deg)
`No Err`	100 %	10^{-5}	`0.023 - 0.005`	`0.038 - 0.001`
`No Err`	100 %	$5 \cdot 10^{-5}$	`0.113 - 0.030`	`0.191 - 0.002`
`Err 1`	100 %	10^{-5}	`0.023 - 0.004`	`0.046 - 0.001`
`Err 1`	100 %	$5 \cdot 10^{-5}$	`0.113 - 0.030`	`0.193 - 0.002`
`Err 2`	18.7 %	10^{-5}	`0.092 - 0.001`	`0.164 - 0.001`
`Err 2`†	99.6 %	$5 \cdot 10^{-5}$	`0.121 - 0.016`	`0.250 - 0.001`

In Table 2 we summarise the results for the different Monte Carlo simulations. Again, for each simulation we show the % of trajectories that remain close to the nominal Halo orbit after 20 orbital revolutions and the maximum and minimum variations on the two angles defining the sail orientation. The first two lines show the results when we do not consider errors during the simulations. The other four lines are for simulations considering errors in the position and velocity determination as well as errors on the sail orientation. `Err 1` shows the results for $\epsilon_\alpha = \epsilon_\delta = 0.001°$ and `Err 2` the results for $\epsilon_\alpha = \epsilon_\delta = 0.01°$.

Again we see that the maximum variation of the sail orientation is related to ε_{max}. But notice that for $\varepsilon_{max} = 5 \cdot 10^{-5}$ the maximum variation of the sail orientation is smaller than the one used for a low Halo orbit (see Table 1). We recall that here the dynamics is less sensitive in small variations to the sail orientation than in the previous case. This is one of the reasons why the control around these orbits is more robust than in the other case.

As before, we include some figures to show the control on the sail orientation and the trajectory that the solar sail follows during one simulation, with and without errors. As before, the errors on the sail orientation are $\epsilon_{\alpha,\delta} = 0.01°$. Here Figures 12 and 14 show results for a simulation when no errors are taken into account and Figures 13 and 15 show the results for a simulation when errors

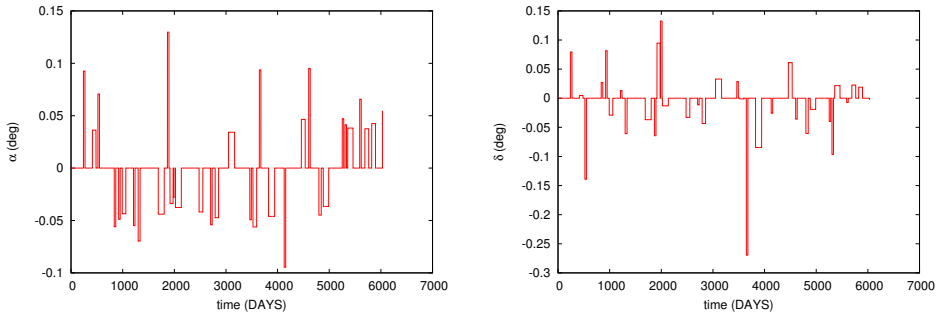

Figure 12. Simulation with no errors for a Halo orbit with $\Delta Z = 800.000$km. Variation of the sail orientation withe respect to time.

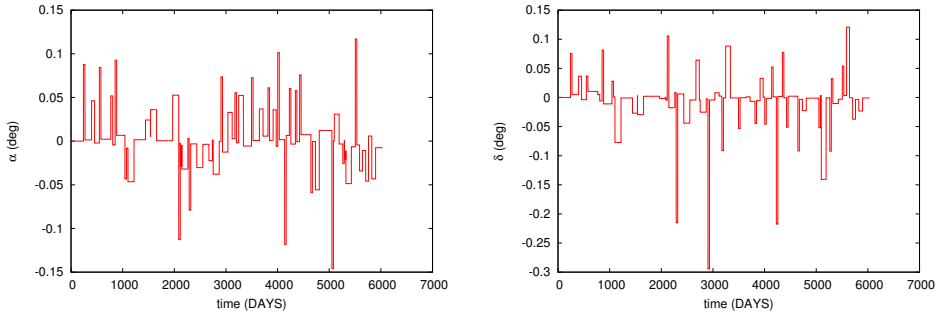

Figure 13. Simulation with errors for a Halo orbit with $\Delta Z = 800.000$km. Variation of the sail orientation withe respect to time.

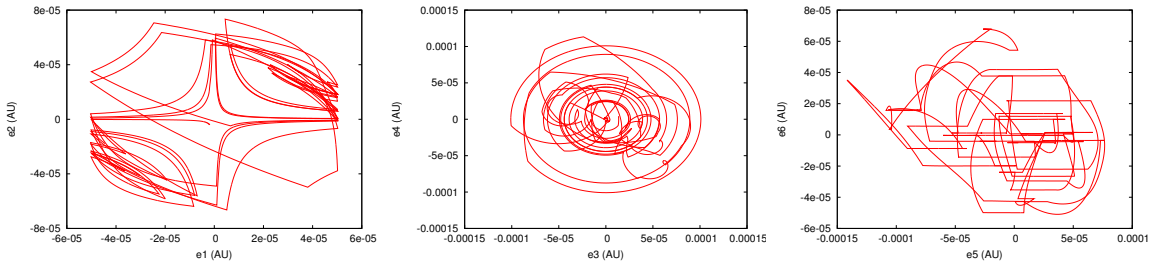

Figure 14. Simulation with no errors for a Halo orbit with $\Delta Z = 800.000$km. Trajectory in the Floquet reference system: Saddle projection $\{\bar{e}_1(\tau), \bar{e}_2(\tau)\}$ (left); Centre projection $\{\bar{e}_3(\tau), \bar{e}_4(\tau)\}$ (middle); Neutral projection $\{\bar{e}_5(\tau), \bar{e}_6(\tau)\}$ (right).

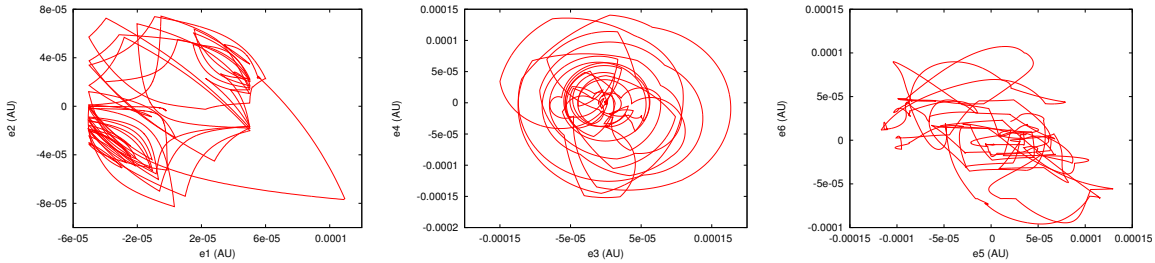

Figure 15. Simulation with errors for a Halo orbit with $\Delta Z = 800.000$km. Trajectory in the Floquet reference system: Saddle projection $\{\bar{e}_1(\tau), \bar{e}_2(\tau)\}$ (left); Centre projection $\{\bar{e}_3(\tau), \bar{e}_4(\tau)\}$ (middle); Neutral projection $\{\bar{e}_5(\tau), \bar{e}_6(\tau)\}$ (right).

are considered.

Figures 12 and 13 show the variation of the sail orientation along time with and without errors. Notice that the average variation for the sail orientation for both angles is always $\approx 0.05°$. The main difference between the simulation when no errors are considered and the one with errors is that in the second case more changes in the sail orientation are required. This is to correct the errors in returning to the nominal orbit induced by the errors on the sail orientation at each manoeuvre.

Figures 14 and 15 show the projection of the trajectory in the Floquet reference system. Notice that the trajectory in the saddle projection $\{\bar{e}_1(\tau), \bar{e}_2(\tau)\}$ is a sequence of saddle connections; the centre projection $\{\bar{e}_3(\tau), \bar{e}_4(\tau)\}$ is a sequence of rotations around different points; and the neutral projection $\{\bar{e}_5(\tau), \bar{e}_6(\tau)\}$ illustrates the drift of the trajectory along the family.

As mentioned above, here the projection of the trajectory in the neutral planes experiences smaller variations than in the previous example. This is mainly due to the fact that small changes on the sail orientation do not derive in big changes on the position of the Halo orbit, having trajectories that remain closer to the nominal orbit.

If we focus on the dynamics on the $\{\bar{e}_1(\tau), \bar{e}_2(\tau)\}$, we see that the different saddle connections of the trajectory always remain within $[-\varepsilon_{max}, \varepsilon_{max}]$, making it more robust to the errors in the sail orientation introduced. We also see that the trajectory in the centre projection remains bounded through all time.

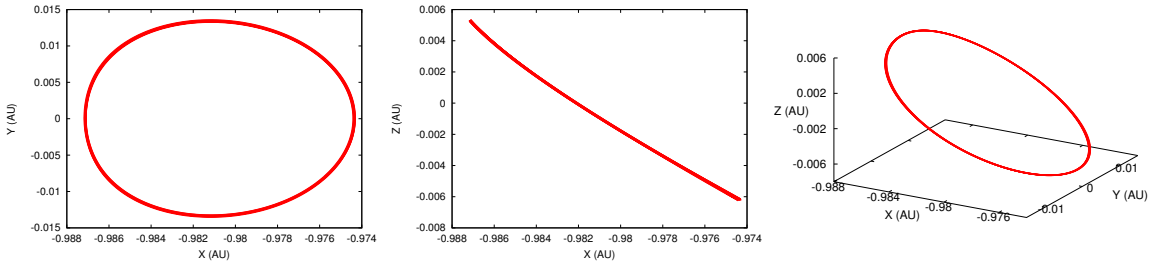

Figure 16. Simulation with errors† for a Halo orbit with $\Delta Z = 800.000$km. Trajectory in the rotation reference system, XY projection (left), XZ projection (middle) and XYZ projection (right).

Finally, Figure 16 shows the trajectory that the sail follows in the position space for the simulation when errors are taken into account. We can see how the trajectory remains close to the Halo orbit for the 20 orbit revolutions of the simulation.

CONCLUSIONS AND FUTURE WORK

In this paper we discuss the controllability of a solar sail around a Halo type orbit close to SL_1 in the Earth - Sun system. We have described the natural dynamics of a solar sail around these objects and how small changes on the sail orientation affect the sails trajectory.

We have also discussed how to use this information to derive efficient station keeping strategies around Halo orbits, and we have derived a station keeping strategy algorithm that we have tested with two examples. We note that this strategy is general enough, and can be used to control the instability of periodic orbits that share similar dynamical properties.

We have considered two Halo orbits for $\beta = 0.05$ and a solar sail perpendicular to the Sun line. The first orbit has an amplitude of 200.000km and the second one of 800.000km. From our results

we can say that low Halo orbits are less controllable than high Halo orbits. The natural dynamics around low Halo orbits is more sensitive to small variations on the sail orientation, making it harder to find appropriate changes that keep the trajectory close to a nominal Halo orbit.

We have also tested the robustness of these strategies introducing systematic errors in the position and velocity determination during the simulations, as well as errors in the sail orientation each time a manoeuvre is done. The most relevant errors in the simulations are those on the sail orientation. From our results we see that high Halo orbits supports larger errors on the sail orientation than low Halo orbits.

A more systematic study on the controllability of these orbits still has to be done. But the strategies presented here have proved their robustness and are a good methodology to deal with the station keeping around these orbits.

ACKNOWLEDGEMENT

This work has been supported by the MEC grant MTM2009-09723 and the CIRIT grant 2009 SGR 67.

REFERENCES

[1] A. McInnes, "Strategies for Solar Sail Mission Design in the Circular Restricted Three-Body Problem," Master's thesis, Purdue University, August 2000.

[2] T. Watters and C. McInnes, "Periodic Orbits above the ecliptic plane in the solar sail restricted 3-body problem," *Journal of Guidance, Control and Dynamics*, Vol. 30, 2007, pp. 786–793.

[3] C. McInnes, *Solar Sailing: Technology, Dynamics and Mission Applications*. Springer-Praxis, 1999.

[4] A. Farrés and À. Jorba, "Dynamical System Approach for the Station Keeping of a Solar Sail," *The Journal of Astronautical Science*, Vol. 58, April–June 2008, pp. 199 – 230.

[5] A. Farrés and À. Jorba, "On the Station Keeping of a Solar Sail in the Elliptic Sun - Earth system," *Advances in Space Research*, Vol. 48, 2011, pp. 1785–1796.

[6] E. Morrow, D. Scheeres, and D. Lubin, "Solar Sail Orbit Operations at Asteroids: Exploring the Coupled Effect of an Imperfectly Reflecting Sail and a Nonspherical Asteroid," *AIAA/AAS Astrodynamics Specialist Conference and Exhibit*, Monterey, California, 2002.

[7] D. Lawrence and S. Piggott, "Solar Sailing Trajectory Control for Sub-L1 Stationkeeping," *AIAA 2004-5014*, 2004.

[8] L. Rios-Reyes and D. Scheeres, "Robust Solar Sail Trajectory Control for Large Pre-Launch Modelling Errors," *2005 AIAA Guidance, Navigation and Control Conference*, August 2005.

[9] V. Szebehely, *Theory of orbits. The restricted problem of three bodies*. Academic Press, 1967.

[10] C. McInnes, A. McDonald, J. Simmons, and E. MacDonald, "Solar Sail Parking in Restricted Three-Body System," *Journal of Guidance, Control and Dynamics*, Vol. 17, No. 2, 1994, pp. 399–406.

[11] A. Farrés, *Contributions to the Dynamics of a Solar Sail in the Earth - Sun System*. PhD thesis, Universitat de Barcelona, October 2009.

[12] M. B. Sevryuk, *Reversible Systems*, Vol. 1211 of *Lecture Notes in Mathematics*. Berlin: Springer-Verlag, 1986.

[13] J. Lamb and J. Roberts, "Time-reversal symmetry in dynamical systems: a survey," *Phys. D*, Vol. 112, No. 1-2, 1998, pp. 1–39.

[14] A. Farrés and À. Jorba, "Periodic and Quasi-Periodic motions of a Solar Sail around the family SL_1 on the Sun - Earth System," *Celestial Mechanics and Dynamical Astronomy*, Vol. 107, 2010, pp. 233–253.

[15] J. Crawford, "Introduction to bifurcation theory," *Reviews of Modern Physics*, Vol. 64, Oct. 1991.

[16] G. Gómez, J. Llibre, R. Martínez, and C. Simó, *Dynamics and Mission Design Near Libration Points - Volume I: Fundamentals: The Case of Collinear Libration Points*, Vol. 2 of *World Scientific Monograph Series in Mathematics*. World Scientific, 2001.

[17] C. Simó, G. Gómez, J. Llibre, R. Martinez, and J. Rodriguez, "On the Optimal Station Keeping Control of Halo Orbits," *Acta Astronautica*, Vol. 15, 1987, pp. 391–397.